0026-895X/94/030555-06$03.00/0

MOLECULAR PHARMACOLOGY, 45:555-560

Role of Tyrosine 337 in the Binding of Huperzine A to the Active Site of Human Acetylcholinesterase

YACOV ASHANI, JACOB GRUNWALD, CHANOCH KRONMAN, BARUCH VELAN, and AVIGDOR SHAFFERMAN
Israel Institute for Biological Research, Ness-Ziona 70450, Israel
Received October 12, 1993; Accepted December 7, 1993

SUMMARY

Huperzine A (HUP), a natural, potent, 'slow,' reversible inhibitor of antiacetylcholinesterase (AChE), has been suggested to be superior to antiacetylcholinesterase drugs now being used for management of Alzheimer's disease. To delineate the binding site of human AChE (HuAChE) for HUP, the biochemical constants k_{on}, k_{off}, and K_i were determined for complexes formed between HUP and single-site (Y337F, Y337A, F295A, W286A, and E202Q) or double-site (F295L/F297V) mutants of recombinant HuAChE (rHuAChE). The kinetic and dissociation constants were compared with those obtained for wild-type rHuAChE and AChE from *Torpedo californica*. Results demonstrate that the inhibition of AChE by HUP occurs through association with residues located inside the active site 'gorge,' rather than at the rim of the gorge. Tyrosine at position 337 (Y337) is essential for inhibition of rHuAChE by HUP (K_i = 26 nM). An aromatic array constituted from residues Y337, F295, and probably W86 is likely to offer a multicontact subsite that interacts with the ammonium group and with both the exo- and endocyclic double bond moieties of HUP. Lack of the aromatic side chain in the position homologous to Y337 explains the poor inhibitory potency of HUP toward human butyrylcholinesterase (K_i > 20,000 nM). Replacement of the carboxylate-containing E202 by glutamine had only marginal effect on the stability of the complex formed between HUP and rHuAChE. The pH-rate profiles suggest that destabilization of the complex after proton gain cannot be attributed solely to protonation of E202. These findings are expected to establish HUP as a lead compound for the design of new anti-AChE drugs.

HUP (Fig. 1) (1), an alkaloid isolated from the club moss Lycopodium *Huperzia serrata*, has been recently characterized as a 'slow' ($k_{on} \approx 1 \times 10^6$ M^{-1} min^{-1}) reversible inhibitor of AChE (EC 3.1.1.7) (2). HUP has attracted considerable interest because of its unique anti-AChE potency (1, 2) and pharmacokinetic properties (3, 4). It was suggested that HUP might be a better therapeutic drug than anti-AChEs such physostigmine, neostigmine, pyridostigmine, or tetrahydroaminoacridine (tacrine), now being used for the alleviation of symptoms related to Alzheimer's dementia, myasthenia gravis, and glaucoma (Refs. 1, 3, and 4 and references cited therein).

An interesting feature of HUP is that, although it displays tight binding to AChEs from mammals (K_i = 20–40 nM) and forms a 5–10-fold less stable complex with TcAChE (K_i = 215 nM), it is >1000-fold less potent as an inhibitor of BChE (EC 3.1.1.8) (2). It was suggested (2) that these differences may be attributed to the variations in the number, type, and location of aromatic amino acid residues that line the active site 'gorge' of AChE (5) and BChE (6). Docking studies predicted that HUP is likely to form multiple contacts with various amino acids deep inside the active site gorge of TcAChE (7, 8). Recent molecular modeling suggested that HUP also interacts with amino acids at the entrance to the gorge.[1] However, the relationship between the proposed binding sites of HUP and the inhibition of enzyme activity remains an open question.

Considering the findings described above, and in view of reports describing significant alleviation of clinical symptoms in patients after treatment with HUP (1, 3, 4), this study was undertaken in an attempt to identify the amino acids that control the binding of HUP to HuAChE. The individual rate constants (k_{on} and k_{off}) that determine the rate of approach to the steady state and the dissociation constant (K_i) of the HUP-AChE complex were determined for wild-type rHuAChE and for its single- and double-site mutants. Results were compared with those obtained for TcAChE. This has enabled us to delineate, in part, residues that determine the extent of inhibition of ChEs by HUP and to offer a possible explanation for the remarkable selectivity of HUP.

Materials and Methods

Synthetic (±)-HUP was obtained from Calbiochem (Lucerne, Switzerland). The concentration of stock solutions of HUP in 50 mM

[1] Y. P. Pang and A. P. Kozikowski. Prediction of huperzine A's multiple binding sites in acetylcholinesterase by docking studies. Submitted for publication.

ABBREVIATIONS: HUP, huperzine A; AChE, acetylcholinesterase; HuAChE, human acetylcholinesterase; TcAChE, acetylcholinesterase from *Torpedo californica*; rHuAChE, recombinant human acetylcholinesterase; BChE, butyrylcholinesterase; HuBChE, human butyrylcholinesterase; FBS, fetal bovine serum; MEPQ, 7-(methylethoxyphosphinyloxy)-1-methylquinolinium iodide; ATC, acetylthiocholine; ChE, cholinesterase.

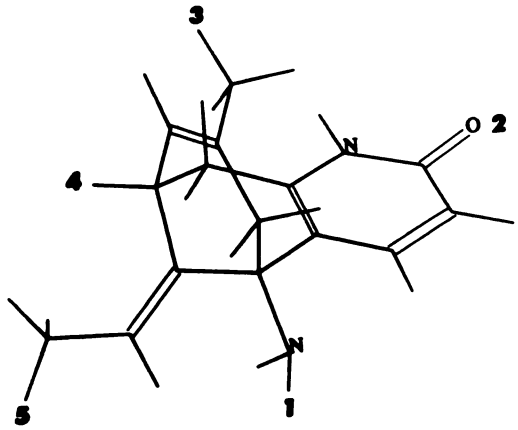

Fig. 1. HUP. The interatomic distances (Å) were extracted from the atomic coordinates reported by Gieb *et al.* (25): atoms 1–3, 6.74; 1–2, 6.99; 1–5, 4.49; 2–3, 6.22; 2–4, 6.85; 2–5, 9.05.

phosphate buffer, pH 8.0, was determined by UV spectroscopy (2). HuBChE was purified from plasma by an affinity chromatography technique to be published elsewhere. Purified TcAChE (solubilized with phosphatidylinositol-specific phospholipase C) was provided by Prof. I. Silman (The Weizmann Institute, Rehovot, Israel). Specific activities were 750 and 3500 units/mg for HuBChE and TcAChE, respectively.

rHuAChE and its mutants. Expression of rHuAChE and its mutants in the human embryonal kidney-derived 293 cell line was described previously (9, 10). Generation of mutants E202Q(E*199*),[2] W286A(W*279*), F295A(F*288*), Y337A(F*330*), and Y337F and the double-mutant F295L(F*288*)/F297V(F*290*) was described elsewhere (11, 12). Wild-type rHuAChE was purified by affinity chromatography (>90% purity, with specific activity of 6000 units/mg) from a high-level expression cell clone culture (13). All mutant enzymes tested (0.1–0.5 units/ml) were collected from the supernatant of stable clone pools (9) containing culture growth medium supplemented with 10% AChE-depleted FBS (10). Spiking of purified rHuAChE with the above diluent did not affect the inhibition characteristic of HUP.

Measurement of AChE activity and determination of the AChE active site concentration. AChE activity was determined in 50 mM phosphate buffer, pH 8.0, at 25° by the method of Ellman *et al.* (14), using 0.5 mM ATC as substrate. Determination of the active site concentration of rHuAChE and TcAChE was carried out through titration with MEPQ (15).

Titration of rHuAChE and TcAChE with HUP. Increasing amounts of HUP (0.1–2.1 times the enzyme equivalents) were added to a 0.005–0.30 μM MEPQ-determined active site concentration of the wild-type enzymes in 5 mM phosphate buffer, pH 8.0. Residual enzyme activity was assayed as described for procedure A.

Determination of biochemical constants. Four protocols were used to determine the dissociation constant K_i and the kinetic rate constants k_{on} and k_{off}, in 50 mM phosphate buffer, pH 8.0, containing 0.02% bovine serum albumin.

In procedure A, a sufficient quantity of HUP was added to produce 20–80% inhibition of 0.1–0.5 units/ml AChE at equilibrium, which was obtained within 2 hr. Residual enzyme activity was determined after 100-fold dilution into the assay cuvette. The initial velocity of the hydrolysis of 0.5 mM ATC was calculated from the slope of the regression line obtained over the first 10–30 sec after dilution into the assay cuvette. In the case of TcAChE, the assay was performed at 14° to minimize dissociation of the diluted HUP-TcAChE complex. K_i was approximated by eq. 1, assuming that equilibrium was obtained in accordance with scheme 1:

$$\text{HUP} + \text{AChE} \underset{k_{off}}{\overset{k_{on}}{\rightleftarrows}} \text{HUP-AChE} \qquad \text{(scheme 1)}$$

$$K_i \approx ([E_f]_{ss}/[E_i]_{ss})[\text{HUP}]_0 \qquad (1)$$

where E_f and E_i are the fractions of active and inhibited enzyme, respectively, and the symbol ss denotes steady state. $[\text{HUP}]_0$ ($\gg[\text{AChE}]_0$) is the initial concentration of HUP.

In procedure B, various amounts of HUP were added to the enzyme solution at $t = 0$ and the rate of approach to steady state was determined after extensive dilution into the assay cuvette at various time intervals. The molar ratio of HUP to AChE was >50. Thus, assuming that k'_{on} (i.e., $k_{on}[\text{HUP}]_0$) and k_{off} are the rate constants of the pseudo-first-order and first-order reactions, respectively (scheme 1), the following equation was derived for the rate of approach to the steady state:

$$E_t = 100e^{-k't} - (E_t)_{ss}(e^{-k't} - 1) \qquad (2)$$

where E_t is percent residual activity at time t, k' is the observed rate constant, and $(E_t)_{ss}$ is the value of E_t at steady state. The individual rate constants k'_{on} and k_{off} were obtained by using eqs. 3 and 4, respectively:

$$k'_{on} = k'[1 - \{(E_t)_{ss}/100\}] \qquad (3)$$

$$k_{off} = k'_{on}(E_t)_{ss}/[100 - (E_t)_{ss}] \qquad (4)$$

In procedure C, K_i values of mutants that formed rapid equilibrium with HUP were calculated by determining the effect of various concentrations of the inhibitor on K_m and V_{max} of the enzyme-catalyzed hydrolysis of ATC. Increasing amounts of ATC were added to a mixture of AChE and HUP that had been preincubated for 10 min in the assay cuvette, and the rate of substrate hydrolysis was determined as described above. The double-reciprocal plot, $1/V$ versus $1/[S]$, provided straight lines. The secondary plot of the slope of each individual line against the concentration of HUP was used to calculate K_i (16).

In procedure D, direct measurement of the rate constant for the dissociation of the complex formed between HUP and either wild-type rHuAChE or TcAChE was initiated by >1000-fold dilution of approximately 0.2 μM AChE that had been allowed to incubate with 0.4 μM HUP for 1 hr. The rate of regeneration of enzyme activity over time was determined as described above. Because the apparent rate constant k'_{on} was negligible, compared with k_{off}, the latter constant was calculated by using the classical integrated form of a first-order reaction equation. The dissociation of the complexes formed with W286A, E202Q, and F295L/F297V was determined as outlined above, after 40–80-fold dilution of pre-equilibrated enzyme-HUP solution into the assay cuvette.

pH-rate profile of the inhibition of rHuAChE by HUP. Values of k'_{on} and k_{off} were determined for the inhibition of rHuAChE by HUP over the pH range of 5.2–8.8, by using protocols B or D. Enzyme solutions (0.3–0.5 units/ml) were made in 0.2 N NaCl-containing buffers prepared from 10 mM acetate (pH 5.2–6.0), phosphate (5.6–8.2), or Tris (7.8–8.8). The pH-rate curves were constructed by nonlinear least squares fitting of the data points in accordance with a single titratable proton, using eq. 5:

$$k_{obs} = k_{max}(1 + \{[H^+]/K_a\})^{-1} \qquad (5)$$

where k_{obs} is either the velocity or the rate constant at a given pH, k_{max} is the $[H^+]$-independent limit of k_{obs}, which corresponds to the fully dissociated acid at high pH (pH − pK_a > 2), and K_a is the dissociation constant of the ionization ($HA \rightleftarrows H^+ + A^-$).

Results

Stoichiometry of the inhibition of AChEs by HUP. The nonlinear curves obtained from the plots of residual AChE activity versus the concentration of HUP (data not shown)

[2] Amino acids and numbers in parentheses refer to the position of the analogous residue in TcAChE, according to the nomenclature recommended by Massoulie *et al.* (24).

were similar to those reported for FBS AChE (2). This indicated that the accumulated complex shifted the equilibrium depicted in scheme 1 to the left.

Calculations (2) showed that 2 mol of HUP were required to inhibit completely the activity of one active site equivalent of either rHuAChE or TcAChE. A similar ratio was reported for the inhibition of FBS AChE by HUP (2). These findings are consistent with the observation that the stereoisomer (−)-HUP is a 38-fold more potent inhibitor of AChE than is the (+)-stereoisomer (17).

Inhibition of wild-type rHuAChE and its mutants by HUP. As shown in Fig. 2, HUP inhibited rHuAChE in a time-dependent manner and the approach to steady state could be reasonably described by eq. 2. The close agreement between k_{off} values that were determined by protocols B and D and the similar dissociation constants (K_i) obtained by direct measurement (procedures A and C) and from the ratio k_{off}/k_{on} (Table 1) support the hypothesis that the extent of the inhibition at equilibrium depends on the forward and reverse reaction rate constants (scheme 1). The observations that the plot of k'_{on} versus the concentration of HUP produced a straight line over inhibitor concentrations ranging from 1 to 10 times the K_i of HUP-rHuAChE (Fig. 2, *inset*) and that k_{off} is independent of the concentration of HUP are consistent with this mechanism. However, the data shown in Fig. 2 cannot rule out the possibility that rapid equilibration of HUP with either a different conformation of the enzyme or a second site precedes the rate-limiting AChE inhibition step.

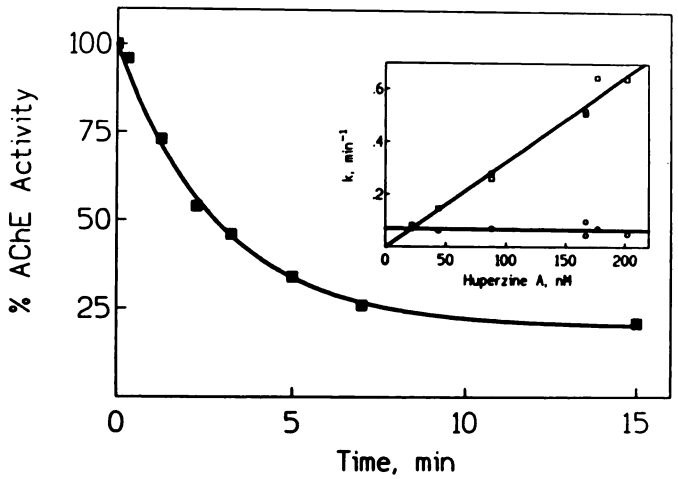

Fig. 2. Time course of the inhibition of wild-type rHuAChE by 88 nM HUP. The curve was computer-fitted to the data points in accordance with eq. 2, and the rate constants k'_{on} (0.28 min^{-1}) and k_{off} (0.07 min^{-1}) were calculated by using eqs. 3 and 4, respectively. *Inset*, plots of k'_{on} (□) and k_{off} (○) versus the concentration of HUP.

TABLE 1

Biochemical constants for inhibition of wild-type rHuAChE and its mutants and TcAChE

Constants were determined in 50 mM phosphate buffer, pH 8.0, at 25°. Values are means ± standard error (four to nine experiments).

AChE (source, mutant)	K_i	$k_{on} \times 10^6$	k_{off}
	nM	$M^{-1}\ min^{-1}$	min^{-1}
rHuAChE			
Wild-type	26 ± 7 (A)[a] 21.6[b]	3.24 ± 0.20 (B)	0.070 ± 0.013 (B)
Y337F	113 ± 30 (C)	NM[c]	NM
Y337A	4900 ± 1300 (C)	NM	NM
F295A	205 ± 40 (A) 156[b]	1.22 ± 0.063 (B)	0.19 ± 0.03 (B)
E202Q	152 ± 17 (A)	0.92[d]	0.14 ± 0.015 (D)
W286A	74 ± 5 (A)	3.51[d]	0.26 ± 0.02 (D)
F295L/F297V	104 ± 15 (A)	3.14[d]	0.33 ± 0.05 (D)
TcAChE, wild-type	143 ± 8 (A) 127[b]	2.98 ± 0.28 (B)	0.38 ± 0.04 (B)

[a] Letters denote method of calculation (see Materials and Methods).
[b] Obtained by dividing k_{off} by k_{on}.
[c] NM, not measured due to rapid equilibration.
[d] Obtained by dividing k_{off} by K_i.

Replacement of Y337 by phenylalanine produced a rHuAChE mutant with a sequence identical to the 14 aromatic residues that line the active site gorge of TcAChE (5, 18) (Table 2). Indeed, the increase of K_i from 26 nM (wild-type rHuAChE) to 113 nM for the Y337F mutant is in good agreement with K_i values obtained for TcAChE (143 and 127 nM) (Table 1). Of all rHuAChE mutants examined, the replacement of tyrosine at position 337 by alanine produced the most dramatic effect on the stability of HUP-rHuAChE. This rapidly formed complex (Fig. 3) was found to be approximately 200-fold less stable than that obtained with wild-type rHuAChE.

In contrast to Y337A, the mutations W286A (at the rim of the active site gorge) and F295A (further down towards the base of the gorge) moderately affected the characteristic ability of wild-type rHuAChE to bind HUP. Thus, K_i values for these

TABLE 2

Differences in the aromatic amino acid residues of the active site gorge of ChEs

Differences were extracted from analysis of the sequence alignment and the three-dimensional structure of TcAChE, as outlined in Ref. 18.

TcAChE	rHuAChE	HuBChE
Tyrosine 70[a]	Tyrosine 72	Asparagine 68[b]
Tyrosine 121	Tyrosine 124	Glycine 119[b]
Tryptophan 279	Tryptophan 286	Alanine 277[b]
Phenylalanine 288	Phenylalanine 295	Leucine 286[b]
Phenylalanine 290	Phenylalanine 297	Valine 288[b]
Phenylalanine 330	Tyrosine 337[b]	Alanine 328[b]

[a] Numbers refer to positions of the indicated amino acids along the sequence of each enzyme (18).
[b] Nonconserved amino acid, relative to TcAChE.

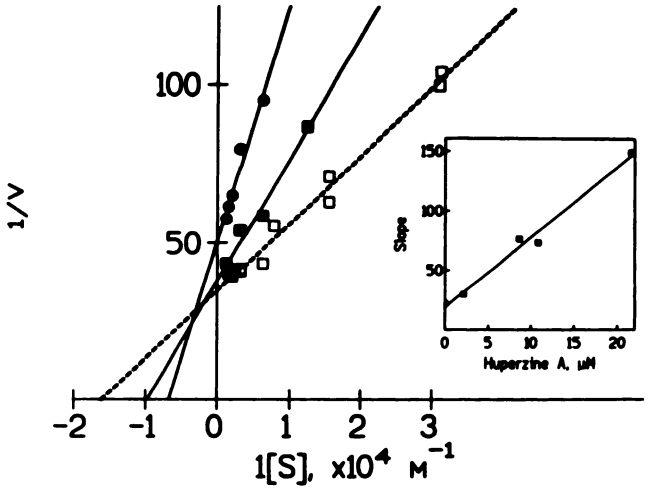

Fig. 3. Plots of 1/*V* versus 1/[S] for the hydrolysis of ATC, [S], by mutant Y337A in the presence of two different concentrations of HUP. □, No HUP; ■, 2.2 μM HUP; ●, 8.2 μM HUP. *Inset*, replot of the slopes of the lines obtained from the double-reciprocal plots versus the concentration of HUP.

mutants were only 3–8-fold higher than that of the wild-type enzyme. The finding that replacement of tryptophan at position 286 by alanine had marginal effects on the stability of the complex with HUP suggests that if HUP interacts with W286[1] this association does not inhibit enzyme activity. Furthermore, the close agreement between the k_{on} of wild-type rHuAChE (measured) and that of W286A (calculated; Table 1) indicates that the indole ring does not interfere with the approach of HUP into its anchoring site.

Aromatic side chain residues F295 (F*288*) and F297 (F*290*) have been recently demonstrated to constitute the pocket that controls the substrate specificity of either HuAChE (12) or mouse AChE (19). Replacement of the two phenylalanines by leucine and valine (F295L/F297V) (Tables 1 and 2) produced an acyl pocket configuration characteristic of HuBChE (12). This double-site modification did not affect significantly the inhibition by HUP (K_i, 104 nM), relative to wild-type rHuAChE. In contrast, no inhibition of HuBChE could be experimentally detected when HUP was present in concentrations as high as 20,000 nM, when either ATC or butyrylthiocholine was used as substrate (data not shown). These findings show that the inability of HUP to associate effectively with HuBChE is not due to the absence of aromatic residues at positions homologous to F295 and F297 in HuAChE.

Mutation of the carboxyl-containing side chain residue E202 that lies at the base of the active site gorge to glutamine (E202Q) slightly destabilized the HUP-AChE complex. The calculated k_{on} for the E202Q mutant (0.92×10^6 M^{-1} min^{-1}) was found to be slightly, but significantly, lower than those obtained for wild-type rHuAChE and TcAChE or mutants W286A and F295/F297A ($2.98–3.51 \times 10^6$ M^{-1} min^{-1}) (Table 1). This observation suggests that the carboxylate side chain of E202 may affect the rate-limiting step of the inhibition of AChE by electrostatic attraction of the positively charged HUP or perturb the formation of a rapid equilibrium between HUP and AChE, which may precede the rate-limiting step.

Effect of pH on k_{on} and k_{off}. The relatively slow inhibition and reactivation permitted us to study separately the effect of pH on the forward and reverse reactions that control formation of HUP-rHuAChE (Fig. 4). The pH-velocity profile of the enzyme-catalyzed hydrolysis of ATC was consistent with an apparent single titratable proton with a pK_a of 6.36 ± 0.05. This pK_a, which is traditionally attributed to the catalytic histidine, is in good agreement with previously reported values (20, 21). A similar relationship was obtained for the pH dependence of the inhibition rate constant k_{on}; however, the data points delineated a titration curve that was slightly shifted to the left, with a pK_a of 5.82 ± 0.10. In marked contrast to the inhibition, the effect of pH on the spontaneous regeneration of enzyme activity, k_{off}, displayed an inverse bell-shaped profile (Fig. 4). Analysis of the effect of pH on k_{off} is more complicated than for k_{on} because the rise of the curve below pH 5.4 may involve partial inactivation of the enzyme. From the curves depicted in Fig. 4, the ratio k_{off}/k_{on} (i.e., the dissociation constant K_i) suggests that the proton gain destabilizes the complex HUP-rHuAChE.

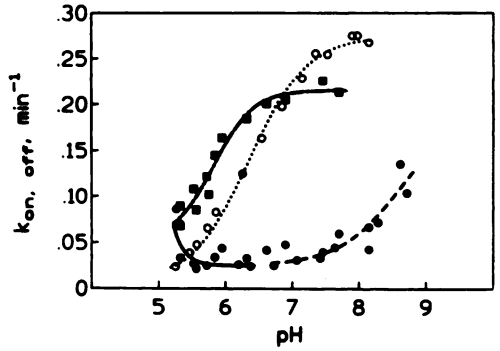

Fig. 4. pH-rate profiles of the rate constants k_{on} (multiplied by 88 nM) (■) and k_{off} (●) for the inhibition of rHuAChE by HUP at 25°. Both protocol B (88 nM HUP) and protocol D (0.22 μM HUP) were used to determine the rate constants. ○, pH-velocity profile of the hydrolysis of ATC (velocity was normalized to fit to the *ordinate* scale).

In the foregoing considerations it has been assumed that neither rHuAChE nor TcAChE forms covalent conjugates with HUP (2). The pH-rate profiles of the inhibition and the spontaneous reactivation of AChEs inhibited by various anti-ChEs that form covalent conjugates (e.g., organophosphates and carbamates) displayed bell-shaped patterns (20). The inverse bell-shaped curve supports the contention (2) that HUP does not acylate the enzyme.

Discussion

HUP is a rigid molecule with an ammonium group at pH <8 and endo- and exocyclic double bonds. The planar 2-pyridone moiety contains two heteroatoms that can associate with amino acids via hydrogen bonds. The distances among these moieties (Fig. 1) are relatively fixed in space by the conformational constraints of the tricyclic ring system. Therefore, HUP might offer a pharmacophore that can produce multiple interactions with various residues inside the gorge of AChEs.

Role of residue Y337 and other amino acids in the association of HUP with AChEs. Of the 14 aromatic residues that project into the catalytic gorge of AChEs (5), six are replaced by aliphatic amino acids in HuBChE (6, 18) (Table 2). Replacement of one of these nonconserved aromatic residues, Y337, with alanine drastically decreased the inhibition by HUP. In contrast, mutation of amino acids W286, F295, and F297 to the corresponding aliphatic residues of HuBChE produced slight to moderate loss in the ability of HUP to inhibit the modified enzyme. These findings, together with the poor anti-HuBChE activity of HUP, suggest that (a) the aromaticity in position 337 is essential for binding of HUP and (b) two of the regions that underlie major differences between AChE and BChE, namely, the peripheral anionic site (W286, in part) (11, 12) and the 'acyl pocket' (positions 295 and 297) (6, 12, 19), are substantially less important than Y337 for the association of HUP with rHuAChE. The role of aromatic residues W*84* and F*330* (homologous to W86 and Y337 in rHuAChE) in the binding of ammonium-containing aromatic ligands inside the active site gorge of TcAChE was recently demonstrated by X-ray diffraction studies of ligand-complexed enzyme crystals (22) and by mutagenesis studies (11, 12). It is not unlikely that the aromatic side chains of residues Y337 and W86 (Fig. 5), the established anionic subsite (11, 12, 22), provide a complementary steric and electronic environment for HUP. We note that, compared with TcAChE, HUP is a 4–6-fold more potent inhibitor of AChEs from either humans, FBS (2), or mouse brain.[3] In these AChEs, F330 of TcAChE is replaced by tyrosine (18). Thus, it is proposed that the electron-donating properties

[3] Y. Ashani and J. Grunwald, unpublished observations.

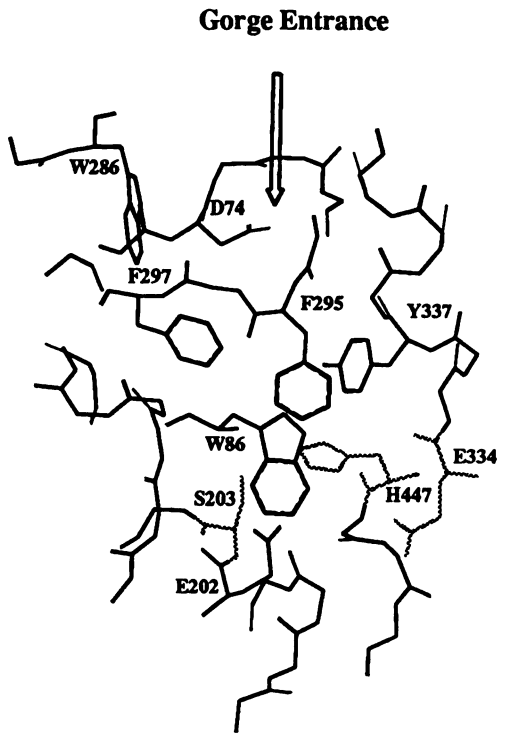

Fig. 5. Cross-sectional view of the active site gorge extracted from a model structure of HuAChE (26). *Labels*, amino acids that were mutated (W286 at the rim and Y337, F295, F297, and E202 within the active site gorge), the catalytic triad (S203, H447, and E334), and residues W86 and D74, located inside and at the entrance to the gorge, respectively. The ammonium group, the exo- and endocyclic bonds, and the bridge methyl group of HUP (see Fig. 1, moieties 1, 5, and 3, respectively) are likely to be clamped by an aromatic array composed of W86, Y337, and F295.

of the hydroxyl group of tyrosine 337 reinforce either π-π or cation-π interactions between HUP and mammalian AChEs.

Once HUP is guided inside the active site gorge and attracted to the π electron-rich Y337, surrounding amino acids such as F295 and E202 can further contribute to the stabilization of the complex. For example, the complex between the F295A mutant and HUP was 8-fold less stable than that formed with wild-type rHuAChE. Regarding the participation of residue E202 in the stabilization of the HUP-AChE complex, computer docking of HUP inside TcAChE suggested that the carboxylate side chain of residue E*199* can either form a hydrogen bond to the pyridone NH (7) or produce a salt bridge with the ammonium group (8). Replacement of the homologous residue in rHuAChE (E202) by the neutral amino acid glutamine resulted in 5-fold destabilization of the complexed enzyme. In view of the existence of more than one ionizable residue in the active site region of AChE, we can only speculate that increasing the pH (i.e., proton removal) is likely to increase the stability of the HUP-AChE complex by one or a combination of the following mechanisms: (a) increasing the concentration of a negatively charged group (e.g., the carboxylate side chain of E202) can stabilize HUP by one of the interactions suggested above (7, 8) and (b) decreasing the concentration of a positively charged residue (e.g., the protonated form of the imidazole side chain of H447) is expected to minimize repulsion of the cation HUP.

Anchoring and orientation of HUP inside the gorge of AChE. The replacement of the pyridone ring with a phenyl moiety decreased the inhibitory potency of HUP by >1000-fold (1). Because the aromaticity of the benzene ring is higher than that of 2-pyridone (23), it is suggested that the latter moiety is projected away from Y337. Thus, the positively charged ammonium group, together with either the endocyclic or the exocyclic double bonds, is likely to interact with Y337 and possibly with W86 (Fig. 5), whereas the pyridone ring heteroatoms are probably utilized to form hydrogen bonds with amino acids distal to Y337.

The results are consistent, in part, with the model proposed by Pang and Kozikowski (7),[1] predicting that the ammonium group and the exoethylidene moiety interact with residues W*84* and F*330* of TcAChE and the pyridone heteroatoms form hydrogen bonds with neighboring amino acid residues. Our data further suggest that the aromatic amino acid F295(F*288*) participates in the stabilization of the HUP-rHuAChE complex. The latter residue may interact with both the endocyclic bond and the bridge methyl group.

The use of rHuAChE mutants permitted the first demonstration that HUP inhibits HuAChE through association within the active site gorge. These findings should be invaluable for establishing HUP as a lead compound for the design and development of improved anti-AChE drugs suitable for management of memory impairment related to deficiency in cholinergic neurons.

Acknowledgments

We thank Dr. D. Barak and Dr. A. D. Wolfe for reviewing the manuscript.

References

1. Kozikowski, A. P., Y. Xia, E. R. Reddy, W. Tuckmantel, I. Hanin, and X. C. Tang. Synthesis of huperzine A and its analogues and their anticholinesterase activity. *J. Org. Chem.* **56**:4636–4645 (1991).
2. Ashani, Y., J. O. Peggins, and B. P. Doctor. Mechanism of inhibition of cholinesterases by huperzine A. *Biochem. Biophys. Res. Commun.* **184**:719–726 (1992).
3. Tang, X. C., P. De Sarno, K. Sugaya, and E. Giacobini. Effect of huperzine A, a new cholinesterase inhibitor, on the central cholinergic system of rat. *J. Neurosci. Res.* **24**:276–285 (1989).
4. Laganiere, S., J. Corey, X. C. Tang, E. Wulfert, and I. Hanin. Acute and chronic studies with the anticholinesterase huperzine A: effect on central nervous system cholinergic parameters. *Neuropharmacology* **30**:763–768 (1991).
5. Sussman, J. L., M. Harel, F. Frolow, C. Oefner, A. Goldman, L. Toker, and I. Silman. Atomic structure of acetylcholinesterase from *Torpedo californica*: a prototype acetylcholine-binding protein. *Science (Washington D. C.)* **253**:872–879 (1991).
6. Harel, M., J. L. Sussman, E. Krecji, S. Bonn, P. Chanal, J. Massuolie, and I. Silman. Conversion of acetylcholinesterase to butyrylcholinesterase: molecular modelling and mutagenesis. *Proc. Natl. Acad. Sci. USA* **89**:10827–10831 (1992).
7. Pang, Y. P., and A. P. Kozikowski. Topography of the huperzine binding site in AChE: *ab initio* docking of reversible inhibitors into the dynamic enzyme, in *Proceedings of the 9th European Symposium on Structure-Activity Relationship and Molecular Modelling.* (1992).
8. Saxena, A., N. Qian, I. M. Kovach, Y. Ashani, A. P. Kozikowski, and B. P. Doctor. Inhibition of cholinesterases by stereoisomers of huperzine A, in *Proceedings of the 1993 Medical Defense Bioscience Review*, Vol. 3. U.S. Army Medical Research and Development Command, Aberdeen Proving Ground, Aberdeen, MD., 1015–1022 (1993).
9. Velan, B., H. Grosfeld, C. Kronman, M. Leitner, Y. Gozes, A. Lazar, Y. Flashner, D. Marcus, S. Cohen, and A. Shafferman. The effect of elimination of intersubunit disulfide bonds on the activity, assembly, and secretion of recombinant human acetylcholinesterase. *J. Biol. Chem.* **266**:23977–23984 (1991).
10. Shafferman, A., C. Kronman, Y. Flashner, M. Leitner, H. Grosfeld, A. Ordentlich, Y. Gozes, S. Cohen, N. Ariel, D. Barak, M. Harel, I. Silman, J. L. Sussman, and B. Velan. Mutagenesis of human acetylcholinesterase. *J. Biol. Chem.* **267**:17640–17648 (1992).
11. Shafferman, A., B. Velan, A. Ordentlich, C. Kronman, H. Grosfeld, M. Leitner, Y. Flashner, S. Cohen, D. Barak, and N. Ariel. Substrate inhibition of acetylcholinesterase: residues affecting signal transduction from the surface of the catalytic center. *EMBO J.* **11**:3561–3568 (1992).
12. Ordentlich, A., D. Barak, C. Kronman, Y. Flashner, M. Leitner, Y. Segall, N. Ariel, S. Cohen, B. Velan, and A. Shafferman. Dissection of the human

acetylcholinesterase active center determinants of substrate specificity: identification of residues constituting the anionic site, the hydrophobic site, and acetyl pocket. *J. Biol. Chem.* **268**:17083–17095 (1993).
13. Kronman, C., B. Velan, Y. Gozes, M. Leitner, Y. Flashner, A. Lazar, D. Marcus, T. Sery, Y. Papier, H. Grosfeld, S. Cohen, and A. Shafferman. Production and secretion of high levels of recombinant human acetylcholinesterase in cultured cell lines: microheterogeneity of the catalytic subunit. *Gene* **21**:295–304 (1992).
14. Ellman, G. L., K. D. Courtney, V. Andres, Jr., and R. M. Featherstone. A new and rapid colorimetric determination of acetylcholinesterase activity. *Biochem. Pharmacol.* **7**:88–95 (1961).
15. Levy, D., and Y. Ashani. Synthesis and *in vitro* properties of a powerful quaternary methylphosphonate inhibitor of acetylcholinesterase. *Biochem. Pharmacol.* **35**:1079–1085 (1986).
16. Segel, I. H. *Biochemical Calculations*. John Wiley & Sons, New York (1976).
17. McKinney, M., J. H. Miller, F. Yamada, W. Tuckmantel, and A. P. Kozikowski. Potencies and stereoselectivities of enantiomers of huperzine A for inhibition of rat cortical acetylcholinesterase. *Eur. J. Pharmacol.* **203**:303–305 (1991).
18. Cygler, M., J. D. Schrag, J. L. Sussman, M. Harel, I. Silman, M. K. Gentry, and B. P. Doctor. Relationship between sequence conservation and three-dimensional structure in large family of esterases, lipases, and related proteins. *Protein Sci.* **2**:366–382 (1993).
19. Vellom, C. D., Z. Radic, Y. Li, N. A. Pickering, S. Camp, and P. Taylor. Amino acid residues controlling acetylcholinesterase and butyrylcholinesterase specificity. *Biochemistry* **32**:12–17 (1993).
20. Aldrich, W. N., and E. Reiner. *Enzymes Inhibitors as Substrates*. North-Holland Publishing Co., Amsterdam (1972).
21. Selwood, T., S. R. Feaster, M. J. States, A. N. Pryor, and D. Quinn. Parallel mechanism in acetylcholinesterase-catalyzed hydrolysis of choline esters. *J. Am. Chem. Soc.* **115**:10477–10482 (1993).
22. Harel, M., I. Schalk, L. Ehret-Sabatier, F. Bouet, N. Goldner, C. Hirth, P. H. Axelsen, I. Silman, and J. L. Sussman. Quaternary ligand binding to aromatic residues in the active site gorge of acetylcholinesterase. *Proc. Natl. Acad. Sci. USA* **90**:9031–9035 (1993).
23. Tieckelmann, H. Pyridinols and pyridones, in *Pyridine and Its Derivatives* (R. A. Abramovitch, ed.), Part 3. John Wiley & Sons, New York, 597–1180 (1974).
24. Massoulie, J., J. L. Sussman, B. P. Doctor, H. Soreq, B. Velan, M. Cygler, R. Rotundo, A. Shafferman, I. Silman, and P. Taylor. Acetylcholinesterase catalysis: protein engineering studies, in *Multidisciplinary Approaches to Cholinesterase Function* (A. Shafferman and B. Velan, eds.). Plenum Publishing Co., New York, 285–288 (1992).
25. Gieb, S. J., W. Tuckmantel, and A. P. Kozikowski. Huperzine A: a potent acetylcholinesterase inhibitor of use in treatment of Alzheimer's disease. *Acta Crystallogr. C* **47**:824–827 (1991).
26. Barak, D., N. Ariel, B. Velan, and A. Shafferman. Molecular models for human AChE and its phosphonylation products, in *Multidisciplinary Approaches to Cholinesterase Functions* (A. Shafferman and B. Velan, eds.). Plenum Publishing Co., New York, 195–199 (1992).

Send reprint requests to: Yacov Ashani or A. Shafferman, Israel Institute for Biological Research, Ness-Ziona 70450, Israel.